Band structures of periodic porphyrin nanostructures

Article

Accepted Version

Band Structures of Periodic Porphyrin Nanostructures

*Victor Posligua[†], Alex Aziz[†], Renée Haver[‡], Martin D. Peeks[‡], Harry L. Anderson[‡], and Ricardo Grau-Crespo[†]**

[†]Department of Chemistry, University of Reading, Whiteknights, Reading RG6 6AD, UK.

[‡]Department of Chemistry, University of Oxford, Chemistry Research Laboratory, Oxford OX1 3TA, UK.

E-mail: r.grau-crespo@reading.ac.uk

Abstract

Recent progress in the synthesis of π-conjugated porphyrin arrays of different shapes and dimensionalities motivates us to examine the band structures of infinite (periodic) porphyrin nanostructures. We use screened hybrid density functional theory simulations and Wannier function interpolation to obtain accurate band structures of linear chains, 2D nanosheets and nanotubes made of zinc porphyrins. Porphyrin units are connected by butadiyne (C4) or ethyne (C2) linkers, or "fused" (C0), i.e. with no linker. The electronic properties exhibit strong variations with the number of linking carbon atoms (C0/C2/C4). For example, all C0 nanostructures exhibit gapless or metallic band structures, whereas band gaps open for the C2 or C4 structures. The

reciprocal space point at which the gaps are observed also show fluctuations with the length of the linkers. We discuss the evolution of the electronic structure of finite porphyrin tubes, made of a few stacked six-porphyrin rings, towards the behavior of the infinite nanotube. Our results suggest approaches for engineering porphyrin-based nanostructures to achieve target electronic properties.

Introduction

Many natural light-harvesting systems are made of cyclic arrays of chlorophyll units.[1] One approach to study the energy and electron transfer processes in natural photosynthesis is based on the use of artificial model systems consisting of porphyrin arrays, which mimic the natural systems.[2] The geometry and dimensionality of such arrays strongly affect the efficiency and rate of photophysical processes. The investigation of porphyrin arrays is also interesting for potential technological applications. For example, large porphyrins arrays attached to semiconductors such as TiO_2 can lead to highly efficient dye-sensitized solar cells,[3] and porphyrin-based molecular wires are being explored in the context of single-molecule electronics.[4-8]

A wide range of porphyrin arrays with different dimensionalities have been synthesized and characterized. Linear chains where porphyrin units are linked via butadiyne (C4) or ethyne (C2), or completely fused (C0), are well studied due to their interesting optical and charge transport properties.[9-14] In particular C0-linked porphyrin chains are known to exhibit very low optical excitation gaps which rapidly decrease as the chains become longer, leading to their very high conductance between metal electrodes.[11] Fused (C0) tetrameric porphyrin "sheets" have been synthesized,[15] and the corresponding limit of a 2D crystal, with vanadium at the porphyrin centers, has been studied theoretically in terms of electronic and magnetic behavior.[16] Cyclic arrays (nanorings) of six,[17] eight,[18] or twelve[19] C4-linked porphyrin units (labeled *c*-**P6**, *c*-**P8** and *c*-**P12**, respectively) have been obtained by template-directed synthesis. It was observed that cyclic

nanorings had lower optical excitation energies than the corresponding linear polymers. Recently, C2-linked nanorings have been synthesized, which exhibit stronger electronic coupling between the porphyrin units.[20] Covalently stacking two *c*-**P6** nanorings results in a "tube" (*t*-**P12**), whose optical absorption spectrum is red-shifted with respect to the individual *c*-**P6** nanorings, reflecting increased conjugation.[21] In the limit of many stacked nanorings, such structures can be seen as one-dimensional nanotubes, with continuous electronic bands. Allec *et al.* have theoretically considered the band structure of C4-linked infinite nanotubes, predicting large oscillations in their band gaps as a function of radius (or number of porphyrin units in the circumference).[22]

Here, we theoretically investigate a range of periodic porphyrin nanostructures in order to predict their structural and electronic properties. We consider linear chains, 2D nanosheets and nanotubes made of Zn-centered porphyrins, and show that their properties exhibit strong variations with the number of carbon atoms (C0/C2/C4) linking the porphyrin units.

Methods

Our simulations were carried out using the VASP code,[23-24] which solves the Schrödinger equation using three-dimensional periodic boundary conditions. Thus, our models are periodic even in the directions in which the nanostructures themselves are non-periodic (Figure 1). Vacuum regions separating the nanostructures are always of at least 12 Å, to minimize the interaction. The linear chains and the nanosheets were contained in an orthorhombic cell, whereas the periodic nanotubes were contained in a hexagonal cell, to conserve the six-fold rotation symmetry along the nanotube axis.

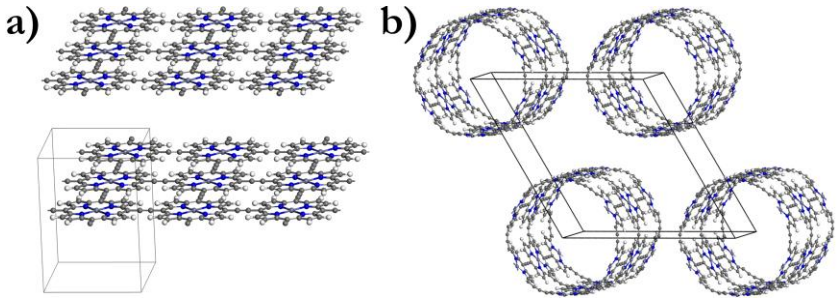

Figure 1. Periodic boundary conditions and unit cells employed in our DFT simulations for a) nanosheets and b) nanotubes.

For geometry optimizations, the exchange and correlation potential was treated within the generalized gradient approximation (GGA) using a dispersion-corrected Perdew-Burke-Ernzerhof functional (PBE-D2).[25-26] In order to obtain accurate electronic structures, we carried out single-point calculations using the screened hybrid functional developed by Heyd, Scuseria and Ernzerhof (HSE06),[27-28] since GGA functionals are known to underestimate the band gap (E_g).[29] HSE06 calculations give E_g values in much closer agreement with experiment than GGA functionals.[30-31] Although the HSE06 calculations were single-point only (no geometry optimization), we tested (for the simpler nanostructures) that the final electronic structures, based on the PBE-D2 optimized structures, were unaffected if the optimization was also conducted at HSE06 level. This is consistent with our previous work modelling the electronic structure of porphyrin-based metal-organic frameworks.[32-33] Γ-centered grids of *k*-points were used for integrations in the reciprocal space. For the nanosheets we use a 6×6×1 mesh, while for the linear chains and the nanotubes we use a 1×1×6 mesh. In order to obtain good-quality band structures and density of state curves, we use an interpolation procedure based on maximally-localized Wannier functions, as implemented in the Wannier90 code.[34] This is important because of the significant band dispersion in the investigated nanostructures, and the huge computational cost of increasing the density of *k*-point

grids in hybrid functional calculations. The interaction of valence electrons with the atomic cores was modeled using projector augmented wave (PAW) potentials, with core levels up to C 1*s*, N 1*s* and Zn 3*p* kept frozen in the atomic reference configurations. For the HSE06 band structure calculations, the kinetic energy cutoff of the plane-wave basis set expansion was set at 400 eV, the recommended value for the chosen PAW potentials. For the PBE-D2 geometry optimizations the cutoff energy was increased by 30% to avoid Pulay errors in the optimized cell parameters.

We have reported all the electron energies with respect to the vacuum reference. As in other periodic DFT codes, the band energies in VASP are given with respect to an internal energy reference. Therefore, to obtain absolute energy levels it was necessary to evaluate the electrostatic potential in a pseudo-vacuum region, given by an empty space within the simulation cell. This was chosen as a planar average in the vacuum gap between nanosheets, and as a spherical average around a point of zero-potential gradient, along the nanotube axis. A Python code provided by Butler *et al*.[35] was employed for this purpose.

Results and Discussions

Porphyrin linear chains

Linear chains are the simplest case of porphyrin arrays. We built flat models (Figure 2, left) consisting of periodic arrays of fused (C0), ethyne-linked (C2) or butadiyne-linked (C4) porphyrin units, and optimized their geometric degrees of freedom. Resulting cell parameters and some relevant bond distances are listed in Table 1.

Table 1. Optimized geometric parameters of the porphyrin linear chains. The parameter *a* is the lattice constant in the periodic dimension.

	C0	C2	C4
$d[C_{meso} - C_{meso}]$ (Å)	1.46	4.04	6.61
$d[C_{\beta} - C_{\beta}]$ (Å)	1.43	4.04	6.59
d[Zn – N] (Å)	2.04	2.05	2.05
Cell length a (Å)	8.42	11.00	13.57

The band structures of these 1D nanostructures are shown in Figure 2 (right). In all cases, both the conduction and valence bands of the polymers exhibit significant dispersion. Whereas the C2 and C4 chains exhibit band gaps of 1.0 eV and 1.1 eV, respectively, the C0 chain has a gap that is very close to zero. The top of the valence band and the bottom of the conduction band are nearly degenerate at the X point of the Brillouin zone (we find an energy difference between the bands of only ~9 meV, which is too small to be reliable given the precision of the calculations). Both bands are approximately linear when approaching the X point, resembling the behavior of the valence and conduction bands of graphene near the Dirac point, and suggesting that electrons and holes in this polymer will be nearly massless. These observations call for further theoretical and experimental investigation of electronic transport in this system. It has been experimentally observed that the HOMO-LUMO gap of fused (C0) porphyrin chains rapidly decreases with the number of porphyrins in the chain, and applications as molecular wires have been suggested.[11-12]

The reciprocal space point at which the narrowest gap is obtained changes from the zone border (X) for the C0-chain, to the zone-center (Γ) for the C2-chain, and back to the zone border (X) for the C4-chain. A similar behavior (oscillation of the point of narrowest gap between the zone center and boundary) will be reported for other porphyrin arrays below, so it is useful to explain this behavior in more detail.

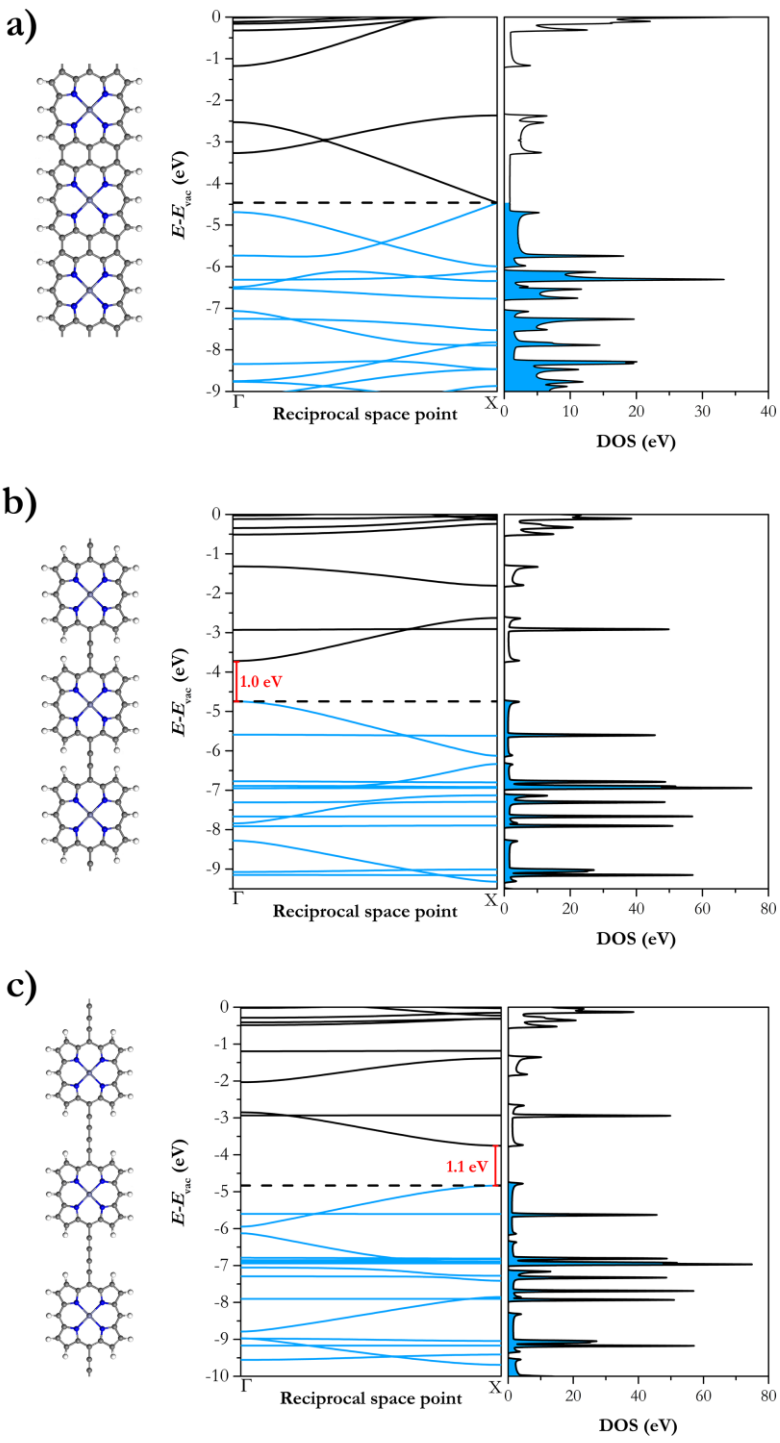

Figure 2. Band structures and density of states of the a) C0-, b) C2-, and c) C4-linked porphyrin linear chains using the HSE06 functional. Energies are given with respect to the vacuum level (E_{vac}). The dashed lines represent the Fermi level; occupied levels are shown in blue.

Figure 3 shows contour plots of the highest-occupied and lowest-unoccupied crystal orbitals (HOCO and LUCO) in the linear chains. The reciprocal space point of these crystal orbitals is related to the relative sign of the wavefunctions at neighboring porphyrin units. In the C0 and C4 linear chains, consecutive porphyrin units have frontier orbitals in antiphase, whereas in the C2 linear chain, they are in phase. This is related to the number of triple bonds in the linker. All the HOCO states have alternating signs on consecutive triple bonds in the linker, while all the LUCO states have alternating signs on consecutive single bonds. Generalizing this result, porphyrin chains with alkyne C*n* linkers can be expected to have in-phase (Γ point) HOCO and LUCO states if the number of triple bonds (*n*/2) is odd and to have anti-phase (zone-boundary) HOCO and LUCO states if *n*/2 is even or zero. We have tested this prediction using linear chains with longer linkers (C6 – C10) and the expected result is confirmed. This behavior is not unique to porphyrin chains; our test calculations lead to the same alternation for linear chains of C*n*-linked benzene units, although in that case the C2 system has HOCO/LUCO at the X point, C4 at the Γ point, etc. (the band structure for the C2 case, the linear phenylacetylene chain, is reported in Ref. [36]). In comparison with the linear benzene chains, our linear porphyrin chains tend to exhibit much narrower gaps.

We now discuss our calculated electronic structure of the porphyrin linear chains in the context of previous theoretical work. Yamaguchi[37] studied this Zn-porphyrin fused tape (C0) using a GGA functional and obtained a zero-gap band structure similar to ours. In contrast, the DFT-based tight-binding (DFTB) calculations of Pedersen *et al.*[38] predicted a band gap of 0.63 eV. Both sets of calculations involve severe approximations, and in particular the GGA is well known to underestimate band gaps, so the prediction of Yamaguchi required confirmation from a more advanced method. Our calculations using a screened hybrid functional indeed confirm that the Zn-

porphyrin C0 linear chain has a zero or near-zero gap. On the other hand, Ohmori *et al.*[39] have also performed hybrid functional (B3LYP) calculations of a similar polymer, but with free-base porphyrins (i.e. 2 H atoms instead of Zn at the porphyrin center). These calculations led to a small band gap (~0.5 eV) which is related to the symmetry breaking by the free-base porphyrins. We have tested that HSE06 calculations indeed lead to a small band gap opening if the Zn is replace by two H atoms at the porphyrin centers. A previous theoretical investigation of the C2-linked infinite linear chain was reported by Susumu *et al*.[40] Despite the simple theoretical model employed in that work (tight-binding model under the Hückel approximation), their band structure (with a bandgap of 1.15 eV) agrees very well with the one reported here at a higher level of calculation.

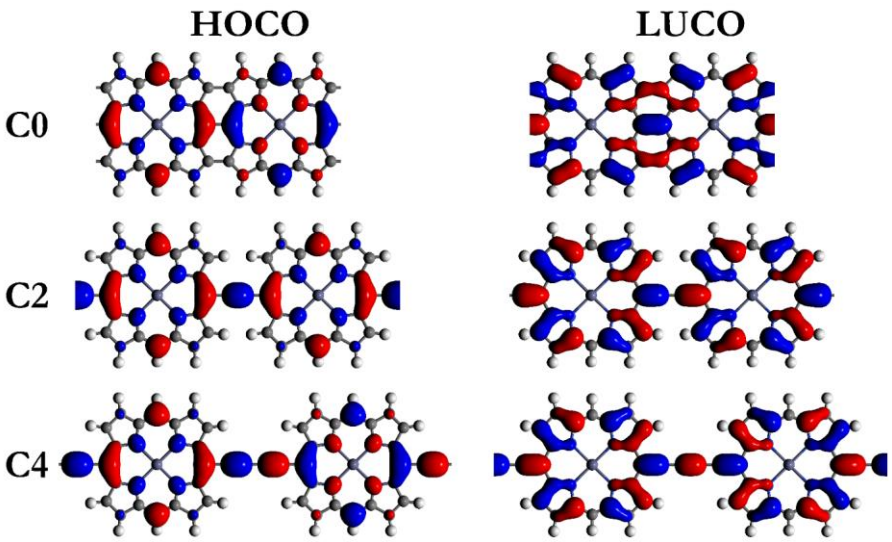

Figure 3. HOCO and LUCO isosurfaces at the Γ (C2 linkage) and X (C0 and C4 linkage) points for porphyrin linear chains. Blue and red represent opposite signs of the wavefunctions.

Porphyrin nanosheets

The optimized geometric parameters of 2D Zn-porphyrin nanosheets with C0, C2, and C4 linkers are shown in Table 2. The results are very similar to those listed in Table 1 for the linear chains.

Table 2. Optimized geometric parameters of the porphyrin nanosheets. The parameter *a* is the lattice constant in the periodic dimensions.

	C0	**C2**	**C4**
$d[C_{meso} - C_{meso}]$ (Å)	1.46	4.07	6.62
$d[C_\beta - C_\beta]$ (Å)	1.41	4.05	6.56
d[Zn – N] (Å)	2.04	2.06	2.06
a (Å)	8.42	11.03	13.55

Figure 4 shows the electronic band structures of the porphyrin nanosheets along the irreducible Brillouin zone defined by the high-symmetry points M, Γ and X in reciprocal space. In the C0-linked nanosheet, the highest-occupied band crosses the Fermi level, implying metallic behavior. On the other hand, both C2-linked and the C4-linked nanosheets (Figure 4b and Figure 4c) exhibit a small band gap. For the C2-linked nanosheet, the narrowest gap is E_g = 0.55 eV at the Γ point, whereas for the C4-linked nanosheet (Figure 4c), the narrowest gap is E_g = 0.31 eV at the M point.

The C0 Zn-porphyrin nanosheets have been theoretically investigated before by Tan *et al.,*[41] and by Yamaguchi,[42] using GGA functionals. Their results agree with ours in predicting a non-spin-polarized ground state with metallic band structure. Our work therefore confirms the absence of band gap to this system, showing that this is not a result of using a GGA functional (which can erroneously predict gapless electronic structures in semiconducting materials). The band structure of the C2 porphyrin nanosheet was calculated by Susumu *et al.* using tight-binding calculations.[40]

Their results are similar to ours, except that they report a wider bandgap (0.79 eV) than us (0.55 eV). Finally, the band structure of the C4 nanosheet has been recently reported by Allec *et al.*[22] using the HSE06 functional and localized basis sets. Our band structure is qualitatively similar to theirs, with a gap opening at the M point, but the band gap obtained by us (0.31 eV) is much narrower than in their work (0.81 eV). Since the same functional is used in both studies, the discrepancy might be due to the different type of basis sets, which requires further investigation.

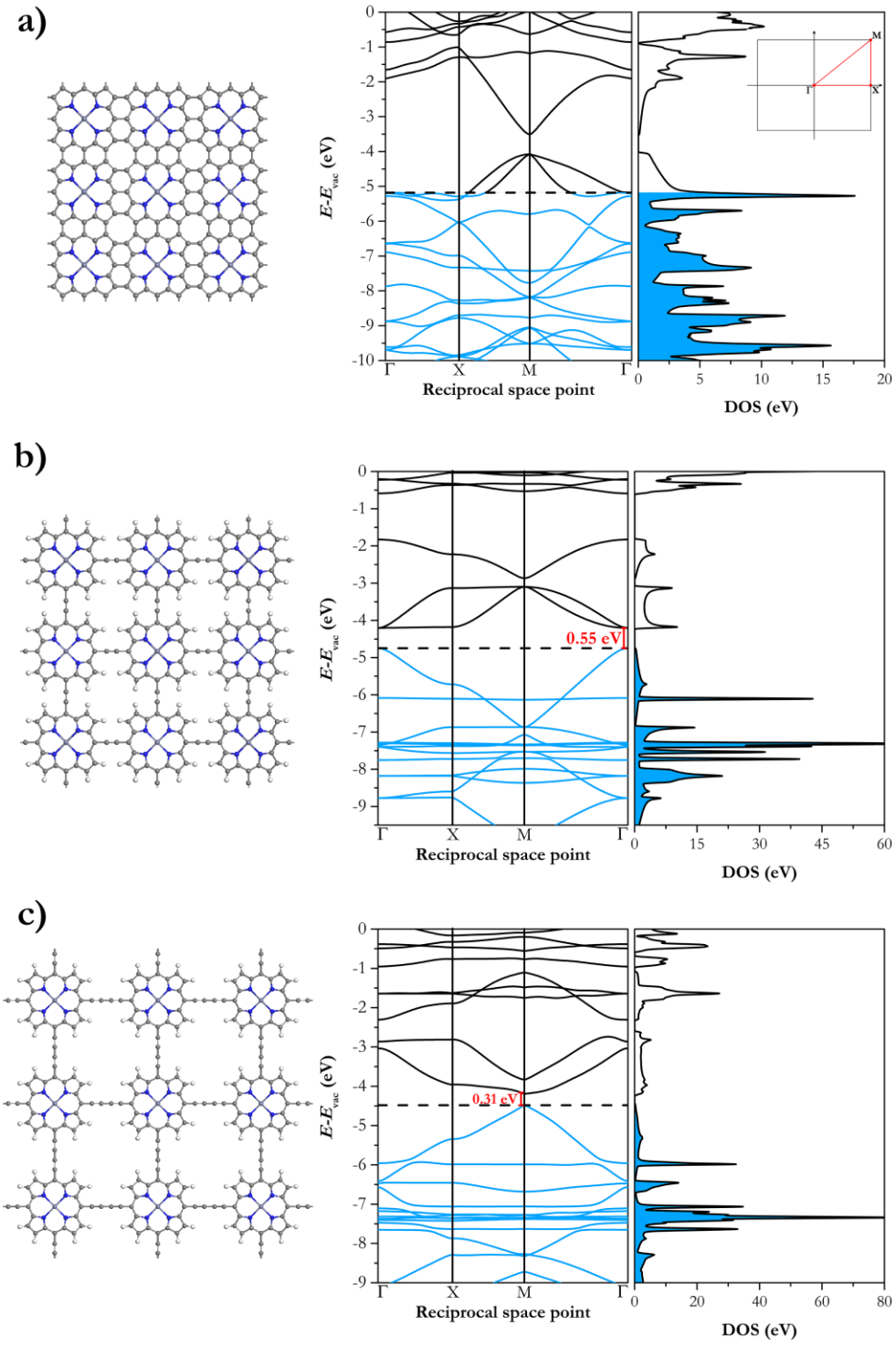

Figure 4. Band structures of the a) C0-, b) C2-, and c) C4-linked porphyrin nanosheets using the HSE06 functional. Energies are given with respect to the vacuum level (E_{vac}). The dashed lines represent the Fermi level; occupied levels are shown in blue.

Porphyrin nanotubes

Porphyrin-based nanotubes are very interesting hypothetical nanostructures, which can be seen as the limit of many stacked porphyrin nanorings.[17-22] We consider here the properties of nanotubes formed by the stacking of nanorings with six porphyrin units, and three types of linkage (C0, C2, C4; Figure 5a-c). We also consider a nanotube with different types of linker: C4 around the ring and C2 along the tube (Figure 5d).

The optimized geometric parameters for all the nanotubes, as well as the strain energies (difference in energy with respect to the corresponding 2D nanosheet) are shown in Table 3.

Table 3. Optimized geometric parameters and strain energies for the porphyrin nanotubes. The parameter *a* is the lattice constant in the periodic direction. Symbols ∥ and ⊥ denote the directions parallel and perpendicular to the tube axis, respectively. The strain energies are obtained using the PBE-D2 functional.

	C0	**C2**	**C4**	**C2/C4**
d[$C_{meso} - C_{meso}\perp$] (Å)	1.45	4.03	6.55	6.61
d[$C_{meso} - C_{meso}\parallel$] (Å)	1.44	4.10	6.59	4.06
d[$C_{\beta} - C_{\beta}\perp$] (Å)	1.37	4.07	6.50	6.57
d[$C_{\beta} - C_{\beta}\parallel$] (Å)	1.40	4.07	6.55	4.05
d[Zn – N] (Å)	2.06	2.04	2.05	2.05
Cell length a (Å)	8.49	11.04	13.54	11.03
Diameter (Å)	15.96	21.04	24.03	25.98
E_{strain} (eV/porphyrin)	0.58	0.29	0.11	0.10

As expected, the strain is highest for the C0 nanotube, as in the absence of linkers the porphyrin units have to accommodate the strain by distorting their planar structure, and becomes lower with longer chains linking the porphyrin units. The strain is lowest when C4 linkers are connecting the porphyrins along the circumference (C4 or C2/C4 nanotubes), whereas the nature of the linker connecting porphyrins along the direction parallel to the nanotube axis is less relevant, as expected.

In order to put the calculated strain energies in context, we have also calculated the strain energies for (6,6) carbon and boron nitride nanotubes at the same level of theory employed here, giving 0.12 and 0.07 eV/atom, respectively. The values in Table 3 for the porphyrin nanotubes correspond to 0.09, 0.04, and 0.02 eV per heavy atom (C or N, i.e. excluding H atoms as they are mono-coordinated and do not contribute to strain) for C0, C2, C4, respectively. Therefore, our porphyrin nanotubes are as or even less strained than typical carbon or boron nitride nanotubes. In terms of geometry, internal bond distances and cell parameters are very similar to those reported for the porphyrin linear chains and nanosheets, with deviations of less than 1.5% in the cell parameter.

The band structures obtained for the porphyrin nanotubes (Figure 5) follow the same pattern as the porphyrin nanosheets: whereas the C0 system is metallic, the presence of the C*n* linkers leads to small band gap openings. The band gaps are 0.50 eV for the C2 nanotube (at the Γ point) and 0.62 eV for C4 nanotube (at the X point). The C2/C4 system has a band gap (0.59 eV) closer to that of the C4 system, but at the Γ point like in the C2 system. This indicates that the reciprocal space position of the narrowest gap is determined by the nature of the linkers along the nanotube axis, which is not surprising given that this is the periodic direction, whereas the magnitude of the gap is mostly determined by the nature of the linkers across the nanotube circumference.

In the semiconducting C*n*-linked nanotubes we observe flat conduction bands, whereas the valence bands exhibit significant dispersion, suggesting much lower effective masses for holes than for conducting electrons. This is in agreement with the work by Allec *et al.,*[22] who calculated the effective hole masses for a series of C4-linked nanotubes with different number of porphyrin units along the tube circumference. Their calculated band gap for the six-porphyrin C4-linked nanotube was 0.77 eV, somewhat wider than our value of 0.62 eV. The same trend was observed above when comparing the band gaps of the C4 nanosheets. Since these authors also employed the

HSE06 functional, the different result is probably due to basis set effects (they employed localized basis sets, which are more difficult to converge than planewave basis sets).

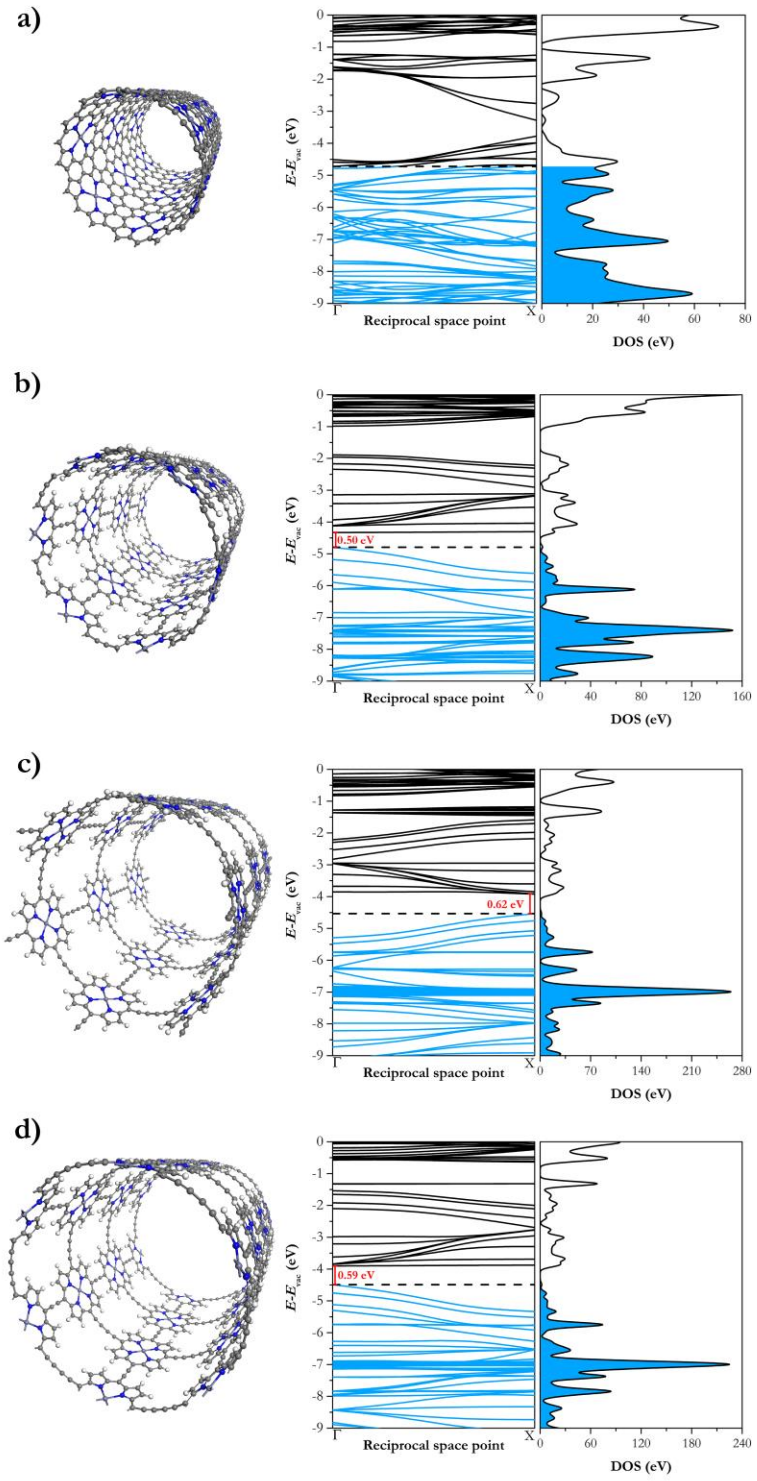

Figure 5. Band structures of the a) C0-, b) C2-, c) C4-, and d) C2/C4-linked porphyrin nanotubes using the HSE06 functional. Electron energies are given with respect to the vacuum level (E_{vac}). The dashed lines represent the Fermi level; occupied levels are shown in blue.

Evolution of electronic structure of nanorings towards the infinite nanotube limit

Whereas actual porphyrin nanotubes have not been synthesized yet, recent progress in stacking porphyrin rings (only two rings so far)[21] suggests that the synthesis of such nanotubes might be feasible. We discuss now how the electronic properties of stacked porphyrin rings vary with the number of rings and converge to the behavior of the infinite 1D nanotube. We consider non-periodic structures consisting of *n* stacked rings (*n* = 1, 2, 3, or 4) of porphyrins connected by C4 linkers. These systems are labeled following the notation in Ref [21]: *c*-**P6** for the cyclic porphyrin hexamer, *t*-**P12** for the "tubular" system consisting of *n* = 2 stacked rings (12 porphyrins in total), *t*-**P18** for *n* = 3, and so on.

The energies of the electronic levels are plotted in Figure 6, showing how the electronic structure tends towards that of the infinite nanotube when *n* increases. The HOMO-LUMO gaps of the finite nanorings are wider than the bandgap of the infinite nanotube, but when the number of stacked rings increases, the gap decreases and tends towards the nanotube bandgap. We find an empirical equation for the band gap variation in the form:

$$E_{\mathrm{g}}(n) = E_{\mathrm{g}}(\infty) + \frac{0.53\ eV}{n^{0.57}} \qquad (1)$$

where $E_{\mathrm{g}}(\infty)$ = 0.62 eV is the band gap for the periodic nanotube (Figure 7). More points would be needed to confirm this trend, but these calculations are very demanding computationally. The current fitting curve suggests that even for a "large" tube of 10 stacked rings, the HOMO-LUMO gap will still be ~0.14 eV above the infinite nanotube limit.

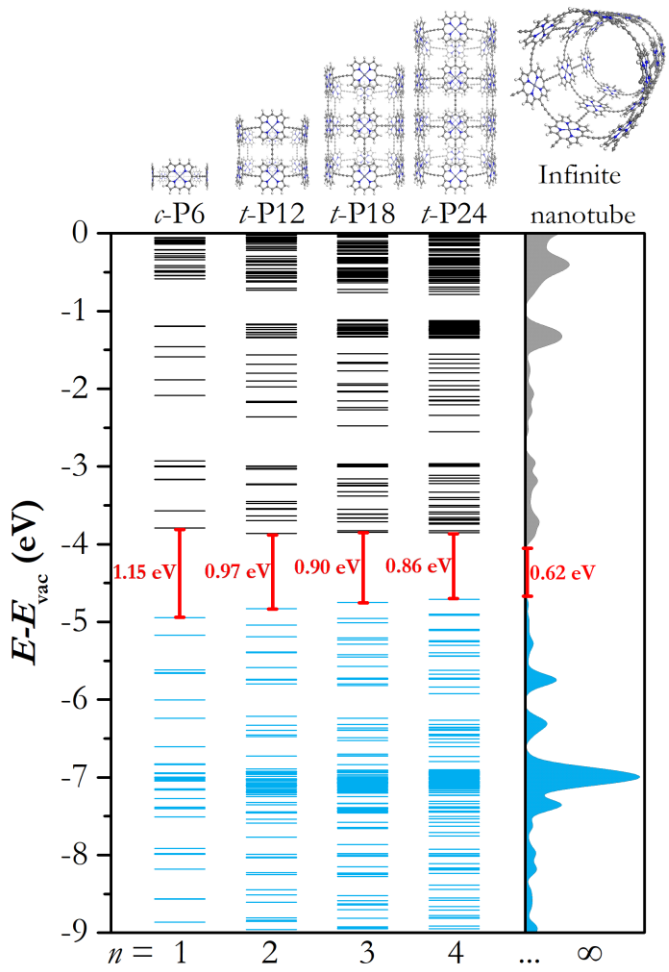

Figure 6. Calculated energy levels of nanorings as a function of the number (*n*) of stacked rings, in comparison with the density of states of the C4-linked nanotube, using the HSE06 functional. Numbers in red are the HOMO-LUMO gap (band gap for the periodic nanostructure). Occupied levels are shown in blue.

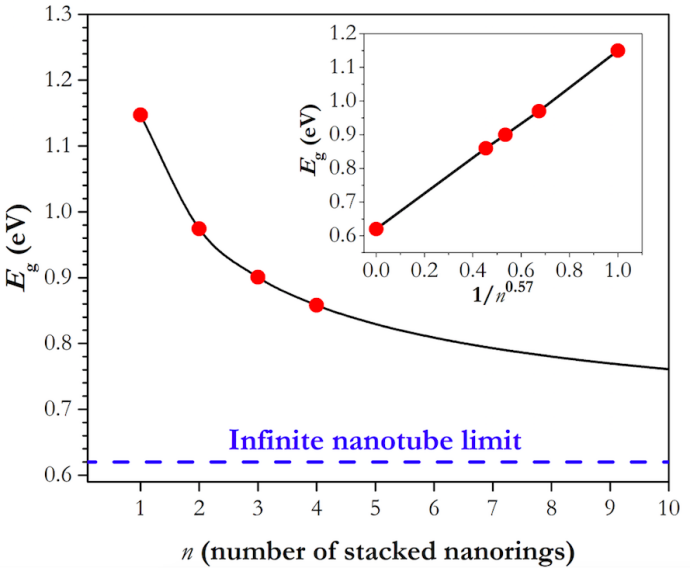

Figure 7. Variation of the HOMO-LUMO gaps of nanorings towards the infinite porphyrin nanotube. *n* is the number of stacked nanorings.

Conclusions

We have performed a systematic investigation of the electronic structure of Zn-porphyrin nanostructures, including linear chains, 2D nanosheets and both finite and infinite nanotubes. In particular, we have investigated the effect of the nature of the linker connecting the porphyrin units, and have observed some strong variations in electronic structure with linker length.

We observed that when the porphyrin units are "fused" (C0 case), there is no band gap in the electronic structure for any of the nanostructures considered here. The C0 nanosheets and nanotubes have metallic band structures, whereas the C0 linear chain (fused porphyrin tape) exhibits a zero-gap band structure with a Dirac-like point at the Brillouin zone boundary.

Narrow band gaps (of ~1 eV or less) open in all nanostructures where the porphyrin units are connected by ethyne (C2) or butadiyne (C4) linkers. The widest opening is observed for the linear chains (1.0 and 1.1 eV for C2 and C4 linkers, respectively), whereas for the nanosheets and

nanotubes the band gaps are significantly narrower (0.3–0.6 eV). Finite porphyrin tubes, made of a few stacked rings, have wider excitation gaps than the infinite (periodic) nanotubes, and we have described the variation of their electronic structures with the number of stacked rings.

The investigated nanostructures exhibit significant band dispersion, suggesting high carrier mobilities. The exception is the conduction bands of the nanotubes, which appear to be remarkably flat. The reciprocal space point at which the band gap is observed is shown to oscillate between the zone center and the zone boundary, depending on the length of the linkers. Neighboring porphyrin units can be expected to be in-phase in the HOCO and LUCO states if the number of triple bonds (n/2) in the linker Cn between them is odd, and in anti-phase if n/2 is even or zero. The narrowest gap in the band structure is observed at the zone center in the former case, and at the zone boundary in the latter case.

Our work theoretically demonstrates that it is possible to design porphyrin nanostructures with tailored electronic properties such as specific band gap values and band structures by varying the type of the linkage used between each porphyrin unit and the type of self-assemble formations (linear chains, nanosheets, nanotubes, and nanorings). These tunable electronic properties represent promising opportunities for light-harvesting or photocatalytic applications.

Acknowledgments

V.P. acknowledges a PhD studentship from the SENESCYT agency in Ecuador. This work made use of ARCHER, the UK's national high-performance computing service, via the UK's HPC Materials Chemistry Consortium, which is funded by EPSRC (EP/L000202). We thank the ERC (grant 320969) for support.

References

1. Cogdell, R. J.; Gall, A.; Köhler, J., The architecture and function of the light-harvesting apparatus of purple bacteria: from single molecules to in vivo membranes. *Q. Rev. Biophys.* **2006,** *39*, 227-324.

2. Nakamura, Y., Aratani, N., Osuka, A., Cyclic porphyrin arrays as artificial photosynthetic antenna: synthesis and excitation energy transfer. *Chem. Soc. Rev.* **2007,** *36*, 831 - 845.

3. Campbell, W. M., Burrell, A. K., Officer, D. L., Jolley, K. W., Porphyrins as light harvesters in the dye-sensitised TiO_2 solar cell. *Coordin. Chem. Rev.* **2004,** *248*, 1363-1379.

4. Crossley, M. J.; Burn, P. L., An approach to porphyrin-based molecular wires: synthesis of a bis(porphyrin)tetraone and its conversion to a linearly conjugated tetrakisporphyrin system. *J. Chem. Soc. Chem. Comm.* **1991**, 1569-1571.

5. Sedghi, G.; García-Suárez, V. M.; Esdaile, L. J.; Anderson, H. L.; Lambert, C. J.; Martín, S.; Bethell, D.; Higgins, S. J.; Elliott, M.; Bennett, N., et al., Long-range electron tunnelling in oligo-porphyrin molecular wires. *Nat. Nanotechnol.* **2011,** *6*, 517.

6. Li, Z.; Park, T.-H.; Rawson, J.; Therien, M. J.; Borguet, E., Quasi-ohmic single molecule charge transport through highly conjugated meso-to-meso ethyne-bridged porphyrin wires. *Nano Lett.* **2012,** *12*, 2722-2727.

7. Kuang, G.; Chen, S.-Z.; Wang, W.; Lin, T.; Chen, K.; Shang, X.; Liu, P. N.; Lin, N., Resonant charge transport in conjugated molecular wires beyond 10 nm range. *J. Am. Chem. Soc.* **2016,** *138*, 11140-11143.

8. Ferreira, Q.; Bragança, A. M.; Alcácer, L.; Morgado, J., Conductance of well-defined porphyrin self-assembled molecular wires up to 14 nm in length. *J. Phys. Chem. C* **2014,** *118*, 7229-7234.

9. Lin, V.; DiMagno, S.; Therien, M., Highly conjugated, acetylenyl bridged porphyrins: new models for light-harvesting antenna systems. *Science* **1994,** *264*, 1105-1111.

10. Susumu, K.; Frail, P. R.; Angiolillo, P. J.; Therien, M. J., Conjugated chromophore arrays with unusually large hole polaron delocalization lengths. *J. Am. Chem. Soc.* **2006,** *128*, 8380-8381.

11. Sedghi, G.; Esdaile, L. J.; Anderson, H. L.; Martin, S.; Bethell, D.; Higgins, S. J.; Nichols, R. J., Comparison of the conductance of three types of porphyrin-based molecular wires: beta-meso, beta-fused tapes, meso-butadiyne-linked and twisted meso-meso linked oligomers. *Adv. Mater.* **2012,** *24*, 653-657.

12. Tsuda, A.; Osuka, A., Fully conjugated porphyrin tapes with electronic absorption bands that reach into infrared. *Science* **2001,** *293*, 79-82.

13. Anderson, H. L., Conjugated porphyrin ladders. *Inorg. Chem.* **1994,** *33*, 972-981.

14. N. Taylor, P.; Huuskonen, J.; T. Aplin, R.; L. Anderson, H.; Huuskonen, J.; Rumbles, G.; Williams, E., Conjugated porphyrin oligomers from monomer to hexamer. *Chem. Commun.* **1998**, 909-910.

15. Nakamura, Y.; Aratani, N.; Shinokubo, H.; Takagi, A.; Kawai, T.; Matsumoto, T.; Yoon, Z. S.; Kim, D. Y.; Ahn, T. K.; Kim, D., et al., A directly fused tetrameric porphyrin sheet and its anomalous electronic properties that arise from the planar cyclooctatetraene core. *J. Am. Chem. Soc.* **2006,** *128*, 4119-4127.

16. Singh, H. K., Kumar, P., Waghmare, U. V., Theoretical prediction of a stable 2D crystal of vanadium porphyrin: a half-metallic ferromagnet. *J. Phys. Chem. C* **2015,** *119*, 25657 - 25662.

17. Hoffmann, M., Kärnbratt, J., Chang, M. H., Herz, L. M., Albinsson, B., Anderson, H. L., Enhanced p conjugation around a porphyrin[6] nanoring. *Angew. Chem.* **2008,** *120*, 5071 - 5074.

18. Hoffmann, M.; Wilson, C. J.; Odell, B.; Anderson, H. L., Template-directed synthesis of a π-conjugated porphyrin nanoring. *Angew. Chem. Int. Ed.* **2007,** *46*, 3122-3125.

19. O'Sullivan, M. C., Sprafke, J. K., Kondratuk, D. V., Rinfray, C., Claridge, T. D. W., Saywell, A., Blunt, M. O., O'Shea, J. N., Beton, P. H., Malfois, M., Anderson, H. L., Vernier templating and synthesis of a 12-porphyrin nano-ring. *Nature* **2011,** *469*, 72 - 75.

20. Rickhaus, M.; Vargas Jentzsch, A.; Tejerina, L.; Grübner, I.; Jirasek, M.; Claridge, T. D. W.; Anderson, H. L., Single-acetylene linked porphyrin nanorings. *J. Am. Chem. Soc.* **2017,** *139*, 16502-16505.

21. Neuhaus, P., Cnossen, A., Gong, J. Q., Herz, L. M., Anderson, H. L., A molecular nanotube with three-dimensional π-conjugation. *Angew. Chem. Int. Ed.* **2015,** *54*, 7344 - 7348.

22. Allec, S. I., Ilawe, N. V., Wong, B. M., Unusual bandgap oscillations in template-directed π-conjugated porphyrin nanotubes. *J. Phys. Chem. Lett.* **2016,** *7*, 2362 - 2367.

23. Kresse, G., Furthmüller, J., Efficiency of ab-initio total energy calculations for metals and semiconductors using a plane-wave basis set. *Comput. Mater. Sci.* **1996,** *6*, 15 - 50.

24. Kresse, G., Furthmüller, J., Efficient iterative schemes for *ab initio* total-energy calculations using a plane-wave basis set. *Phys. Rev. B* **1996,** *54*, 11169 - 11186.

25. Perdew, J. P., Burke, K., Ernzerhof, M., Generalized gradient approximation made simple. *Phys. Rev. Lett.* **1996,** *77*, 3865 - 3868.

26. Perdew, J. P., Burke, K., Ernzerhof, M., Errata: "Generalized gradient approximation made simple [Phys. Rev. Lett. 77, 3865 (1996)]". *Phys. Rev. Lett.* **1997,** *78*, 1396.

27. Heyd, J., Scuseria, G. E., Ernzerhof, M., Hybrid functionals based on a screened Coulomb potential. *J. Chem. Phys.* **2003,** *118*, 8207 - 8215.

28. Heyd, J., Scuseria, G. E., Ernzerhof, M., Erratum: "Hybrid functionals based on a screened Coulomb potential" [J. Chem. Phys. 118, 8207 (2003)]. *J. Chem. Phys.* **2006,** *124*, 219906.

29. Zhu, G., Sun, Q., Kawazoe, Y., Jena, P., Porphyrin-based porous sheet: optoelectronic properties and hydrogen storage. *Int. J. Hydrogen Energy* **2015,** *40*, 3689 - 3696.

30. Henderson, T. M., Paier, J., Scuseria, G. E., Accurate treatment of solids with the HSE screened hybrid. *Phys. Status Solidi B* **2011,** *248*, 767 - 774.

31. Garza, A. J., Scuseria, G. E., Predicting Band Gaps with Hybrid Density Functionals. *J. Phys. Chem. Lett.* **2016,** *7*, 4165 - 4170.

32. Aziz, A., Ruiz-Salvador, R., Hernández, N. C., Calero, S., Hamad, S., Grau-Crespo, R., Porphyrin-based metal-organic frameworks for solar fuel synthesis photocatalysis: band gap tuning via iron substitutions. *J. Mater. Chem. A* **2017,** *5*, 11894-11904.

33. Hamad, S., Hernandez, N. C., Aziz, A., Ruiz-Salvador, A. R., Calero, S., Grau-Crespo, R., Electronic structure of porphyrin-based metal-organic frameworks and their suitability for solar fuel production photocatalysis. *J. Mater. Chem. A* **2015,** *3*, 23458 - 23465.

34. Souza, I.; Marzari, N.; Vanderbilt, D., Maximally localized Wannier functions for entangled energy bands. *Phys. Rev. B* **2001,** *65*, 035109.

35. Butler, K. T., Hendon, C. H., Walsh, A., Electronic chemical potentials of porous metal - organic frameworks. *J. Am. Chem. Soc.* **2014,** *136*, 2703 - 2706.

36. Kondo, M.; Nozaki, D.; Tachibana, M.; Yumura, T.; Yoshizawa, K., Electronic structures and band gaps of chains and sheets based on phenylacetylene units. *Chem. Phys.* **2005,** *312*, 289-297.

37. Yamaguchi, Y., Time-dependent density functional calculations of fully π-conjugated zinc oligoporphyrins. *J. Chem. Phys.* **2002,** *117*, 9688 - 9694.

38. Pedersen, T. G., Lynge, T. B., Kristensen, P. K., Johansen, P. M., Theoretical study of conjugated porphyrin polymers. *Thin Solid Films* **2005,** *477*, 182 - 186.

39. Ohmori, S., Kawabata, H., Tokunaga, K., Tachikawa, H., Molecular design of high performance fused porphyrin one-dimensional wire: a DFT study. *Thin Solid Films* **2009,** *518*, 901 - 905.

40. Susumu, K.; Maruyama, H.; Kobayashi, H.; Tanaka, K., Theoretical approach to the design of supramolecular conjugated porphyrin polymers. *J. Mater. Chem.* **2001,** *11*, 2262-2270.

41. Tan, J., Li, W., He, X., Zhao, M., Stable ferromagnetism and half-metallicity in two-dimensional polyporphyrin frameworks. *RSC Adv.* **2013,** *3*, 7016 - 7022.

42. Yamaguchi, Y., Theoretical study of two-dimensionally fused zinc porphyrins: DFT calculations. *Int. J. Quantum Chem.* **2009,** *109*, 1584-1597.

TOC Graphic